

Supporting Information

Slow Magnetic Relaxation in a Homo Dinuclear Dy(III) Complex in a Pentagonal Bipyamidal Geometry

*Joydev Acharya,^a Naushad Ahmed,^{#b} Jessica Flores Gonzalez,^{#c} Pawan Kumar,^a Olivier Cador,^c Saurabh Kumar Singh,^{*d} Fabrice Pointillart,^{*c} Vadapalli Chandrasekhar^{*a,b}*

Table S1. Crystal data and structure refinement parameters of complexes.

Complex	1	1_Y
Formula*	C ₂₈ H ₃₈ Cl ₄ Dy ₂ N ₆ O ₁₀	C ₂₈ H ₃₈ Cl ₄ N ₆ O ₁₁ Y ₂
g/mol	1085.44	954.26
Crystal system	monoclinic	monoclinic
Space group	<i>C</i> 2/ <i>c</i>	<i>C</i> 2/ <i>c</i>
<i>a</i> /Å	14.9522(7)	14.9090(6)
<i>b</i> /Å	11.4148(7)	11.5451(6)
<i>c</i> /Å	23.0815(12)	22.9371(9)
α (°)	90	90
β (°)	96.781(2)	90.379(4)
γ (°)	90	90
<i>V</i> /Å ³	3911.9(4)	3948.0(3)
<i>Z</i>	4	4
ρ_c /g cm ⁻³	1.843	1.605
μ /mm ⁻¹	4.121	3.256
<i>F</i> (000)	2112.0	1928.0
Crystal size (mm ³)	0.02 × 0.02 × 0.02	0.02 × 0.02 × 0.02
θ range (deg)	4.502 to 56.664	5.464 to 58.02
Limiting indices	-19 ≤ <i>h</i> ≤ 19, -15 ≤ <i>k</i> ≤ 15, -30 ≤ <i>l</i> ≤ 30	-18 ≤ <i>h</i> ≤ 19, -15 ≤ <i>k</i> ≤ 10, -30 ≤ <i>l</i> ≤ 28
Reflns collected	29322	20504
Ind reflns	4882 [R _{int} = 0.0699]	4636 [R _{int} = 0.0343]
Completeness to θ (%)	100	100
Refinement method	Full-matrix least-squares on <i>F</i> ²	Full-matrix least-squares on <i>F</i> ²
Data/restraints/parameters	4882/24/230	4636/12/235

Goodness-of-fit on F^2	1.120	1.105
Final R indices [$I > 2\theta(I)$]	$R_I = 0.0510, wR_2 = 0.1198$	$R_I = 0.0581, wR_2 = 0.1502$
R indices (all data)	$R_I = 0.0768, wR_2 = 0.1348$	$R_I = 0.0715, wR_2 = 0.1553$

* The formula of the complexes are of the entities present in unit cell and are slightly different from actual molecular formula in main text. This is because, two coordinated –OH group in both the complexes and one isolated OH₂ in complex **1Y** have not taken associated hydrogen atoms in crystal structure.

Table S2. Possible geometries around the metal centres and their corresponding ChSM values.

Geometry	Point group	ChSM value around Dy1	ChSM value around Dy2
Heptagon	D_{7h}	33.977	33.977
Hexagonal pyramid	C_{6v}	25.663	25.663
Pentagonal bipyramid	D_{5h}	0.479	0.479
Capped octahedron	C_{3v}	8.200	8.200
Capped trigonal prism	C_{2v}	6.312	6.312
Johnson pentagonal bipyramid J13	D_{5h}	5.813	5.813
Johnson elongated triangular pyramid	C_{3v}	23.786	23.786

Table S3. Bond lengths and bond angles in the **1**.

Description of Bond	Bond Length (Å)	Description of Angle	Bond Angle (°)	Description of Angle	Bond Angle (°)
Dy1---Dy1*	3.6862(6)	O3*—Dy1—N1	141.39(18)	O2—Dy1—O3*	143.07(16)
Dy1—Cl1	2.6113(2)	Cl1—Dy1—Cl2	169.78(6)	O2*—Dy1—O3*	68.59(16)
Dy1—Cl2	2.6266(2)	N1—Dy1—Cl1	89.64(14)	O2—Dy1—N1	75.52(17)
Dy1—O2	2.285(4)	N1—Dy1—Cl2	86.87(14)	O2*—Dy1—N1	150.01(17)
Dy1—O2*	2.345(4)	Dy1—O2—Dy1*	105.51(17)	O2—Dy1—O1	141.71(16)
Dy1—O1	2.351(5)	O2*—Dy1—Cl1	92.18(12)	O1—Dy1—Cl1	84.80(13)
Dy1—O3*	2.350(5)	O2—Dy1—Cl1	93.51(13)	O1—Dy1—Cl2	85.00(13)
Dy1—N1	2.459(6)	O2*—Dy1—Cl2	95.64(12)	O1—Dy1—N1	66.23(17)
		O2—Dy1—Cl2	94.91(13)	O3*—Dy1—Cl1	87.11(14)
		O2—Dy1—O2*	74.49(17)	O3*—Dy1—Cl2	89.63(14)
		O2*—Dy1—O1	143.74(16)	O3*—Dy1—O1	75.17(16)

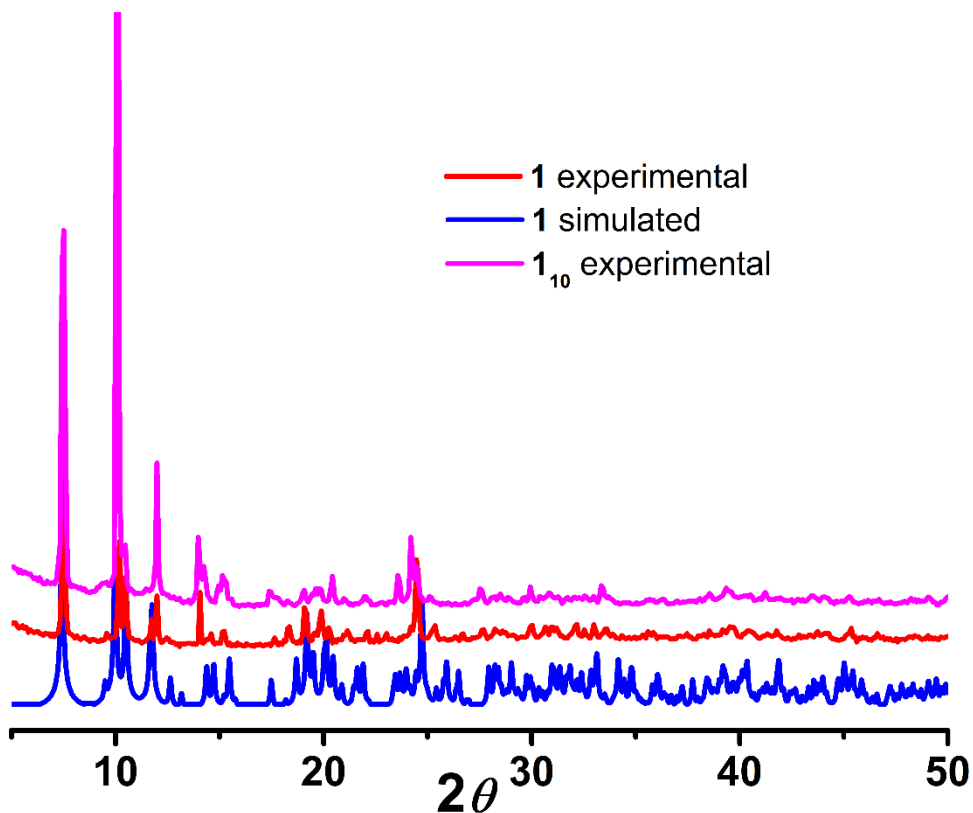


Figure S1. Simulated and experimental XRD pattern for **1** along with experimental pattern of **1₁₀**.

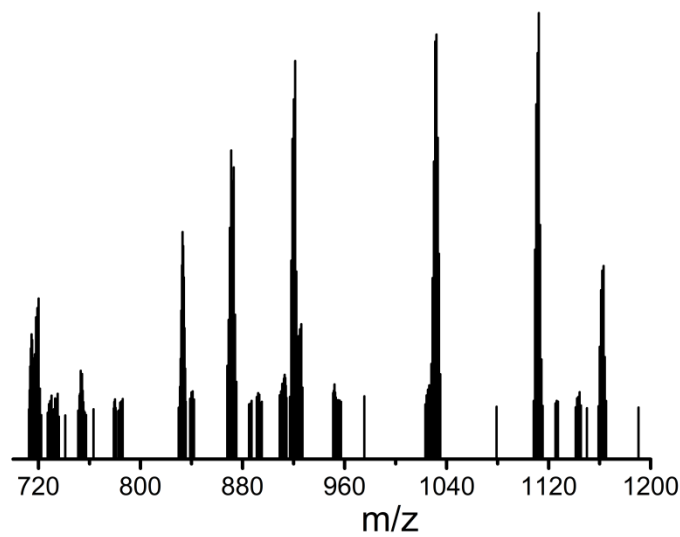


Figure S2. Full range ESI-MS spectra of **1** using MeOH as solvent.

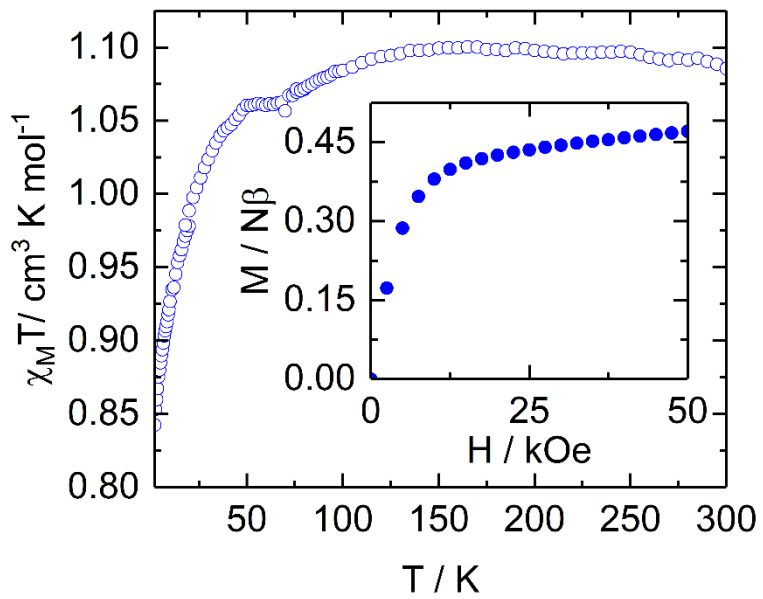


Figure S3. Thermal dependence of the $\chi_M T$ product (open circles) and the inset corresponds to the field dependence of the magnetization at 2 K for $\mathbf{1}_{10}$.

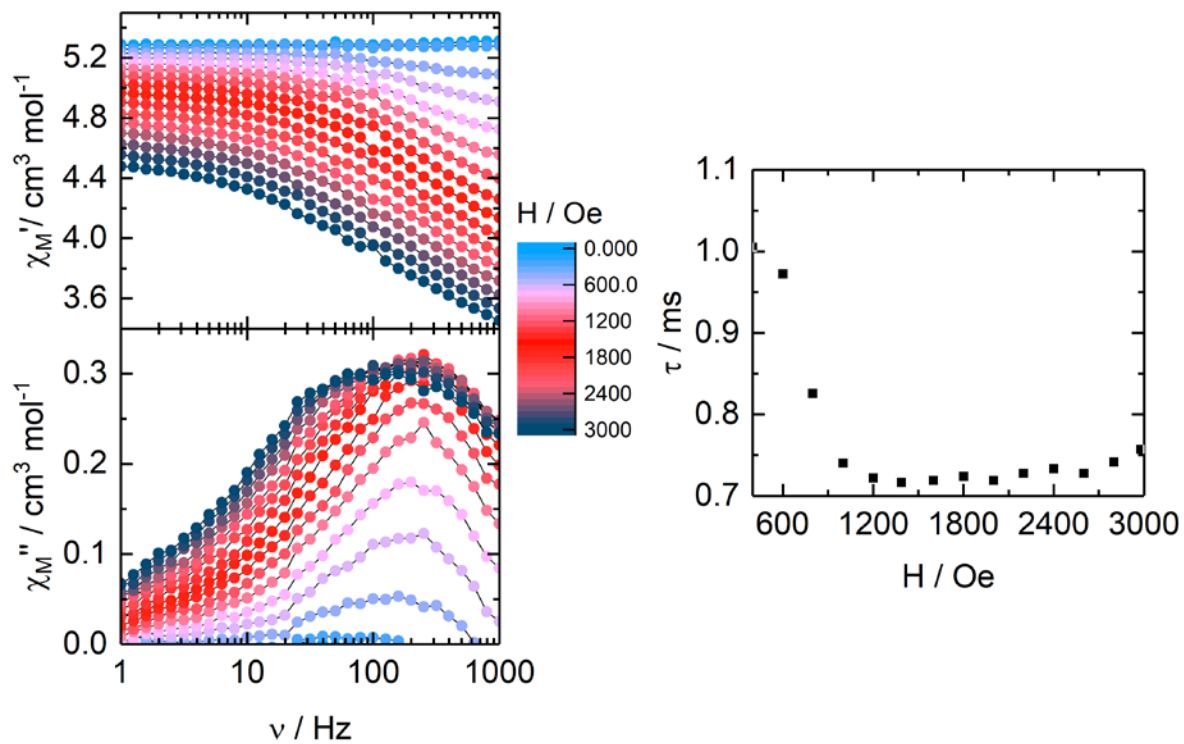


Figure S4. (Left) In-phase and out-of-phase components of the ac magnetic susceptibility for **1** at 2 K in an applied DC magnetic field from 0 to 3000 Oe. (Right) Representation of the field-dependence of the relaxation time of the magnetization at 2 K.

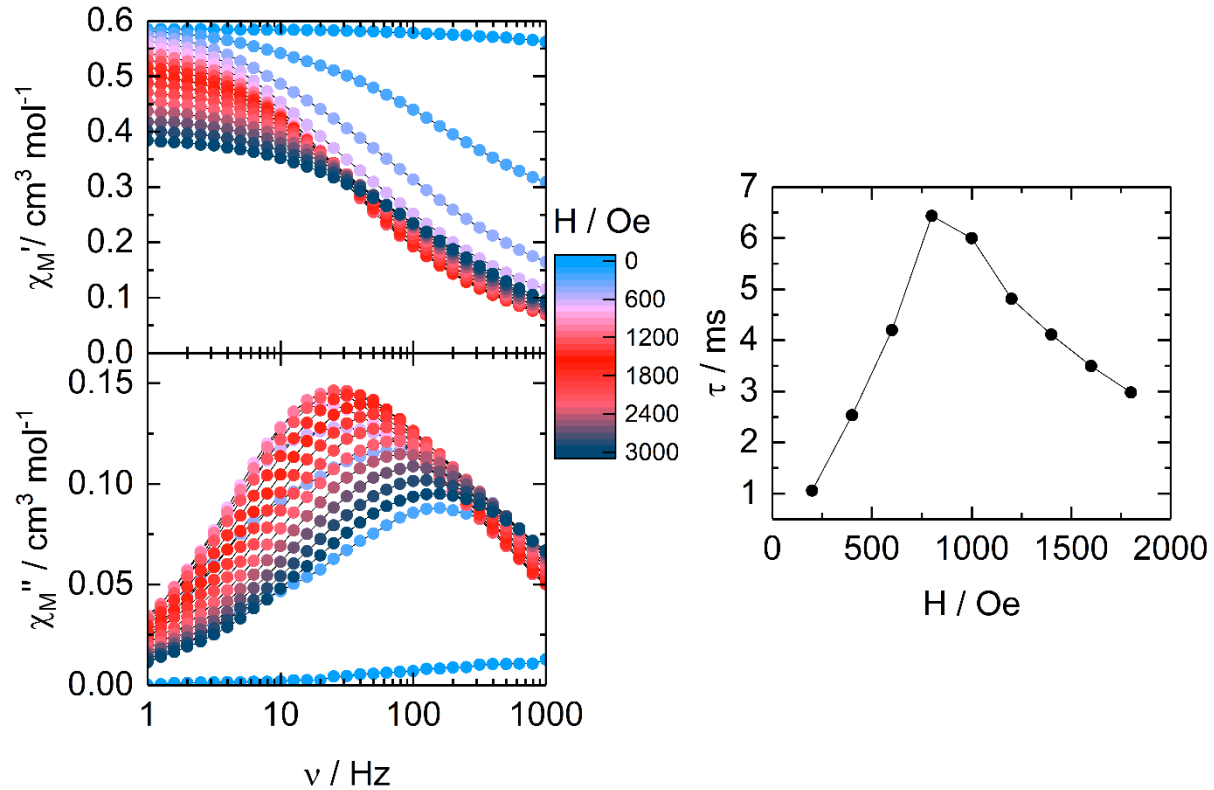


Figure S5. (Left) In-phase and out-of-phase components of the ac magnetic susceptibility for **1₁₀** at 2 K under a DC magnetic field from 0 to 3000 Oe. (Right) Representation of the field-dependence of the relaxation time of the magnetization at 2 K, the maximal τ corresponding to 800 Oe.

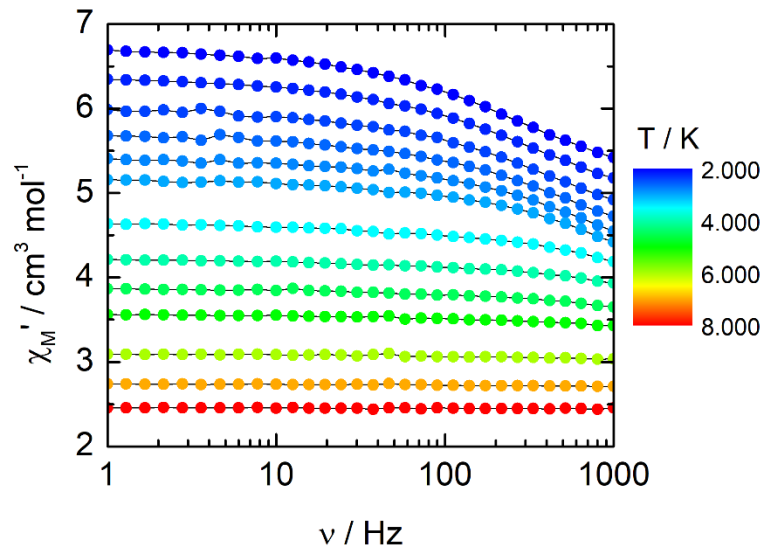


Figure S6. In-phase component of the ac magnetic susceptibility data for **1**, from 2 to 8 K under 1200 Oe.

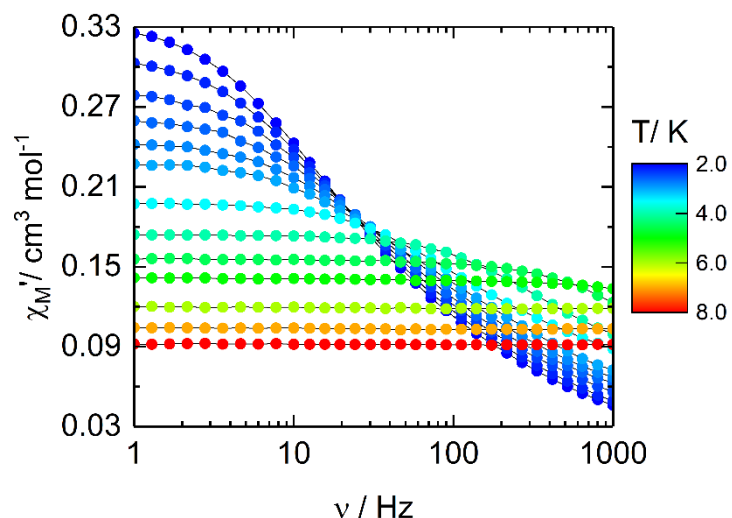


Figure S7. In-phase component of the ac magnetic susceptibility data for **1₁₀**, from 2 to 8 K under 800 Oe.

Extended Debye:

$$\chi_M' = \chi_s + (\chi_t - \chi_s) \frac{1 + (\omega\tau)^{1-\alpha} \sin\left(\alpha \frac{\pi}{2}\right)}{1 + 2(\omega\tau)^{1-\alpha} \sin\left(\alpha \frac{\pi}{2}\right) + (\omega\tau)^{2-2\alpha}}$$

$$\chi_M'' = (\chi_t - \chi_s) \frac{(\omega\tau)^{1-\alpha} \cos\left(\alpha \frac{\pi}{2}\right)}{1 + 2(\omega\tau)^{1-\alpha} \sin\left(\alpha \frac{\pi}{2}\right) + (\omega\tau)^{2-2\alpha}}$$

With χ_t the isothermal susceptibility, χ_s the adiabatic susceptibility, τ the relaxation time and α an empiric parameter which describe the distribution of the relaxation time. For SMM with only one relaxing object α is close to zero. The extended Debye model was applied to fit simultaneously the experimental variations of χ_M' and χ_M'' with the frequency ν of the oscillating field ($\omega = 2\pi\nu$). Typically, only the temperatures for which a maximum on the χ_M'' vs. ν curves, have been considered (see figure here below for an example). The best fitted parameters τ , α , χ_t , χ_s are listed in Table S4 to S6 with the coefficient of determination R^2 .

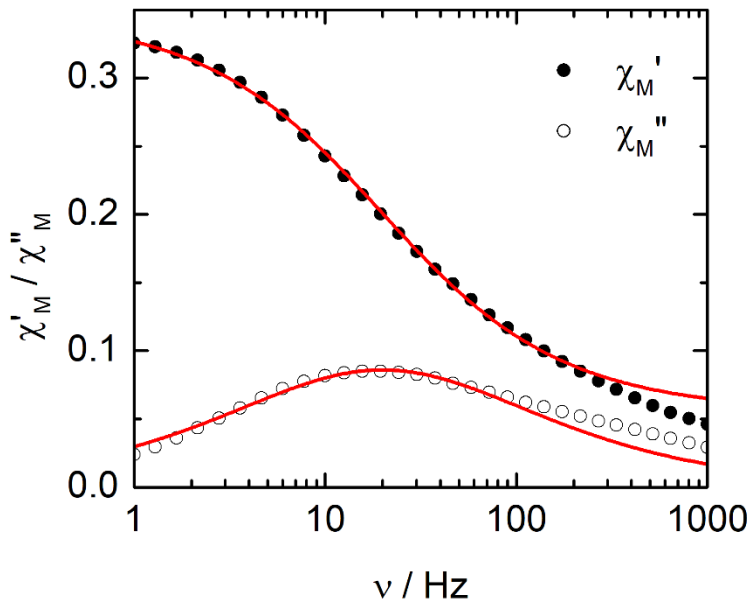


Figure S8. Frequency dependence of the in-phase (χ_M') and out-of-phase (χ_M'') components of the ac susceptibility measured on powder at 2 K and 800 Oe with the best fitted curves (red lines) for $\mathbf{1}_{10}$.

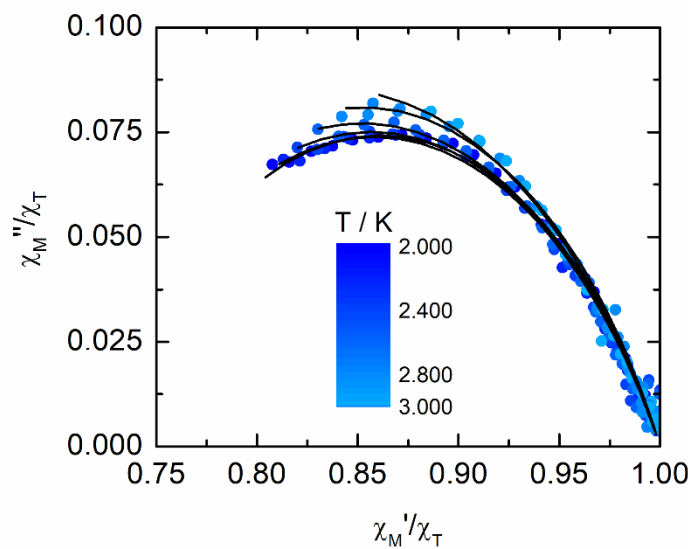


Figure S9. Normalized Cole-Cole plot at several temperatures between 2 and 3 K for **1**.

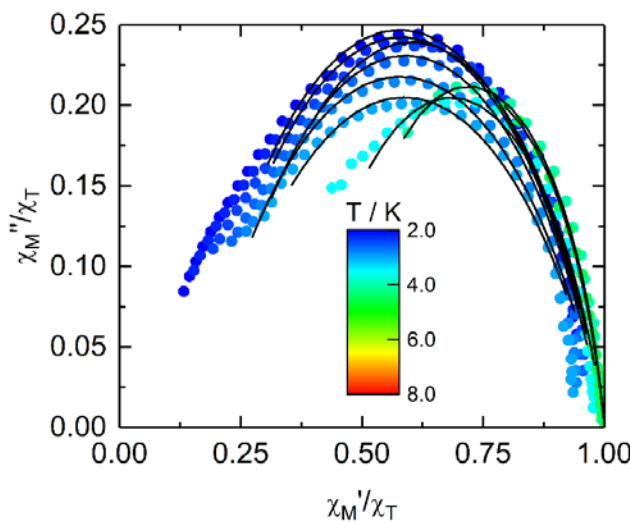


Figure S10. Normalized Cole-Cole plot at several temperatures between 2 and 4.5 K for **1₁₀**.

Table S4. Best fitted parameters (χ_T , χ_S , τ and α) with the extended Debye model for compound **1** at 1200 Oe in the temperature range 2-3 K.

T	$\chi_s / \text{cm}^3 \text{ mol}^{-1}$	$\chi_T / \text{cm}^3 \text{ mol}^{-1}$	τ / s	α	R^2	$(\chi_T - \chi_s)/\chi_T / \%$
2	4.83721	6.69892	4.7560E-04	0.37552	0.99999	27.79
2.2	4.55112	6.35432	3.8877E-04	0.38879	0.99999	28.38

2.4	4.26962	5.98625	3.0983E-04	0.38602	0.99998	28.68
2.6	3.99974	5.68089	2.3303E-04	0.38833	0.99998	29.59
2.8	3.80139	5.3905	1.8291E-04	0.36062	0.99999	29.48
3	3.48796	5.14649	1.1317E-04	0.38144	0.99998	32.22

Table S5. Best fitted parameters (χ_T , χ_s , τ and α) with the extended Debye model for compound **1₁₀** at 800 Oe in the temperature range 2-4.5 K.

T	$\chi_s / \text{cm}^3 \text{ mol}^{-1}$	$\chi_T / \text{cm}^3 \text{ mol}^{-1}$	τ / s	α	R^2	$(\chi_T - \chi_s / \chi_T) / \%$
2	0.05408	0.348	7.9900E-03	0.32607	0.99942	84.46
2.2	0.05205	0.32106	6.2300E-03	0.33193	0.9995	83.79
2.4	0.05991	0.29106	4.9900E-03	0.30904	0.99963	79.42
2.6	0.04919	0.2715	3.3700E-03	0.34585	0.99947	81.88
2.8	0.04037	0.25658	2.3000E-03	0.3921	0.99957	84.27
3	0.0421	0.24264	1.7800E-03	0.41355	0.99948	82.65
3.5	0.07417	0.20185	0.00121	0.26788	0.99971	63.25
4	0.07689	0.17489	4.44E-04	0.17533	0.99994	56.03
4.5	0.06652	0.15589	9.97E-05	0.19265	0.99997	57.33

Table S6. CASSCF computed low-lying 21 sextets and 224 quartets spin-free states for Dy1 centre in complex **1**. All the values are reported here in cm⁻¹. The values in grey colour are for the sextet states while values in the red colour are for the quartet states.

0.0	25389.9	31243.0	43954.1	62738.8	88964.3
6.3	25423.8	31244.1	45184.6	62744.1	88973.7
230.3	25459.9	31259.5	45198.7	62990.9	89235.8
281.5	25492.9	31266.1	45229.8	62990.9	89236.4
286.2	25515.7	31291.3	45269.7	67812.0	99406.5
333.0	25519.4	31316.3	45320.3	67879.1	99479.5
408.8	25551.9	31334.0	45337.9	68094.6	99503.0
410.7	25559.7	31343.4	45338.5	73553.2	99553.2
436.5	25576.4	31350.5	45391.8	73562.5	99582.1
451.4	25585.3	31372.2	45400.0	73735.5	99782.4
493.8	25586.7	31372.2	45472.1	73790.3	99803.9
7612.3	25627.3	33029.0	45474.3	73871.5	106653.2
7681.9	25628.0	33090.7	45482.5	77443.8	106676.9
7707.8	25636.3	33144.2	45484.9	77614.3	106708.4
7735.1	25636.7	33210.2	57644.5	77624.0	106786.7
7768.9	26422.4	33227.6	57645.9	77629.7	106827.9
7858.2	26423.4	34612.2	57668.1	77641.8	106838.1
7893.1	26458.8	34615.6	57680.7	77642.7	106840.4
34843.7	26472.8	34631.3	57690.8	77648.5	106927.7
35085.2	26507.9	34634.5	57702.9	77651.1	106936.2
35164.7	26513.3	34640.0	57712.0	77661.3	
24876.3	26538.6	34650.4	57718.4	77662.2	
24876.9	26542.7	34656.3	57724.3	77727.4	
25016.9	26554.3	34661.2	57768.5	77733.6	
25017.8	29768.8	34666.0	57773.1	79103.4	
25021.5	29769.4	34676.8	57830.8	79155.6	
25039.3	29803.6	34677.5	57843.7	79246.4	
25068.1	29810.8	37678.1	57895.6	79269.9	
25075.9	29818.1	37695.1	57905.7	79283.4	
25076.4	29824.4	37864.6	57913.9	79297.9	
25111.8	29825.8	37926.7	57921.9	79320.3	
25117.8	29835.3	37942.8	57929.5	85920.6	
25146.0	29836.7	37980.2	57966.9	85932.8	
25161.6	29842.7	37996.7	57967.8	85981.9	
25208.1	29848.2	38050.2	62595.4	86161.8	
25264.4	29852.9	38094.7	62602.6	86166.7	
25269.9	29857.0	38120.0	62608.9	88782.6	
25289.8	29871.8	38161.4	62618.5	88788.2	
25307.6	29872.2	38163.9	62645.4	88820.8	
25313.3	31183.3	43535.9	62655.4	88843.5	
25318.8	31186.3	43660.1	62668.6	88877.4	
25331.7	31191.1	43707.9	62713.3	88915.9	
25343.9	31192.2	43746.2	62725.8	88923.6	
25369.8	31211.5	43807.4	62735.9	88946.4	
25380.5	31213.7	43909.4	62738.2	88961.4	

Table S7. CASSCF computed low-lying 21 sextets and 224 quartets spin-free states for Dy2 centre in complex **1**. All the values are reported here in cm⁻¹. The values in grey colour are for the sextet states while values in the red colour are for the quartet states.

0.0	25389.4	31243.1	43954.2	62738.4	88965.2
6.3	25423.1	31244.2	45185.2	62743.5	88973.0
231.4	25460.5	31259.7	45200.0	62991.1	89235.9
283.5	25493.2	31266.3	45228.9	62991.2	89236.5
286.3	25516.1	31291.4	45269.9	67816.1	99407.6
334.3	25519.6	31316.5	45319.8	67874.9	99479.6
406.5	25551.8	31334.1	45338.2	68094.9	99506.1
413.3	25559.8	31343.5	45338.7	73554.0	99550.5
435.2	25576.7	31350.7	45391.5	73562.2	99580.8
450.4	25585.4	31372.3	45400.2	73739.1	99782.0
494.4	25586.9	31372.3	45472.2	73786.9	99803.7
7612.7	25627.5	33029.2	45474.3	73870.8	106653.5
7682.2	25628.3	33090.9	45482.6	77443.8	106678.3
7707.5	25636.7	33144.4	45485.0	77614.5	106706.8
7735.7	25637.1	33210.2	57645.9	77624.0	106786.4
7769.1	26422.6	33227.8	57647.6	77630.4	106827.3
7858.5	26423.6	34612.3	57667.8	77642.0	106838.0
7893.3	26459.0	34615.7	57681.2	77642.9	106840.2
34843.5	26473.4	34631.4	57690.8	77647.7	106927.6
35090.2	26508.2	34634.3	57703.3	77650.4	106935.9
35160.3	26514.2	34640.1	57712.0	77661.3	
24876.4	26539.6	34650.6	57716.9	77662.1	
24877.0	26541.7	34656.6	57723.0	77727.5	
25017.4	26553.4	34661.4	57768.5	77733.7	
25018.8	29768.8	34666.6	57773.0	79102.9	
25021.3	29769.4	34676.9	57831.3	79156.0	
25039.6	29803.9	34677.7	57844.4	79247.2	
25068.4	29811.1	37679.4	57898.3	79270.9	
25076.3	29818.4	37694.0	57906.0	79283.5	
25076.9	29824.6	37864.8	57915.2	79296.8	
25111.5	29826.3	37927.0	57921.8	79319.4	
25117.3	29834.9	37943.0	57930.3	85921.3	
25146.0	29836.2	37980.6	57964.0	85935.8	
25161.4	29843.1	37996.7	57964.8	85978.5	
25208.3	29848.8	38050.1	62596.9	86161.3	
25265.0	29853.6	38095.6	62604.6	86166.6	
25270.4	29857.7	38118.9	62609.5	88783.9	
25289.8	29871.7	38161.5	62619.6	88790.2	
25307.8	29872.2	38164.1	62644.8	88820.7	
25313.3	31183.4	43536.3	62653.9	88843.7	
25319.0	31186.4	43660.2	62668.0	88876.1	
25331.8	31191.2	43707.4	62712.8	88915.7	
25344.1	31192.3	43747.1	62726.1	88922.6	
25370.4	31211.7	43807.2	62735.0	88946.2	
25381.1	31213.9	43909.5	62738.1	88959.9	

Table S8. CASSCF+RASSI-SO computed low-lying 16 spin-orbit states for Dy1 and Dy2 centres in complex **1**. All the values are reported here in cm^{-1} . The SOC states were computed by mixing spin-free states (only 21 sextets, 21 sextets+ 108 quartets).

Dy1		Dy2	
only 21 sextets	21 sextets + 108 quartets	only 21 sextets	21 sextets + 108 quartets
0.0	0.0	0.0	0.0
0.0	0.0	0.0	0.0
241.1	238.7	241.8	239.4
241.1	238.7	241.8	239.4
266.0	263.4	267.5	264.9
266.0	263.4	267.5	264.9
289.3	286.2	289.8	286.8
289.3	286.2	289.8	286.8
349.1	344.8	349.0	344.8
349.1	344.8	349.0	344.8
370.6	364.9	372.7	367.0
370.6	364.9	372.7	367.0
409.2	403.3	407.7	401.8
409.2	403.3	407.7	401.8
424.7	418.1	423.7	417.1
424.7	418.1	423.7	417.1

Table S9. SINGLE_ANISO computed g-values and the angle of deviation from ground state g_{zz} orientation of low-lying eight Kramers doublet for Dy1 centre in complex **1**.

Dy1		
$\pm m_J$ states (from 21 sextets only)	$g_{xx}; g_{yy}; g_{zz}$	
0.0	0.0009; 0.0022; 19.9527	
241.1	2.0659; 2.6069; 14.3496	
266.0	0.9835; 2.4265; 13.2787	
289.3	1.4146; 1.7990; 12.7668	
349.0	0.0790; 3.5802; 10.7643	
370.6	10.3005; 6.3378; 2.1724	
409.3	1.5167; 3.5256; 12.6750	
424.7	0.4508; 4.5382; 13.4310	
$\pm m_J$ states (from 21 sextets+ 108 Quartets only)	$g_{xx}; g_{yy}; g_{zz}$	θ ($^{\circ}$ angle)
0.0	0.0008; 0.0021; 19.8622	0
238.7	1.9391; 2.4122; 14.4857	3.3

263.4	0.8267; 2.2623; 13.4437	86.8
286.2	1.3796; 1.6859; 12.8229	88.7
344.8	0.1254; 3.5191; 10.7466	95.2
364.9	10.2167; 6.4074; 2.1975	94.8
403.3	1.4572; 3.4930; 12.6879	47.3
418.1	0.4590; 4.4646; 13.4192	44.5

Table S10. SINGLE_ANISO computed g-values and the angle of deviation from ground state g_{zz} orientation of low-lying eight Kramers doublet for Dy2 centre in complex **1**.

Dy2		
$\pm m_J$ states (from 21 sextets only)	$g_{xx}; g_{yy}; g_{zz}$	
0.0	0.0009; 0.0023; 19.9687	
241.8	1.9446; 2.2552; 14.6002	
267.5	0.3452; 2.2978; 13.4248	
289.8	1.4365; 1.6922; 12.4383	
349.0	0.3557; 3.4397; 10.6520	
372.7	10.1910; 6.2775; 2.0057	
407.7	1.6932; 3.1898; 12.4472	
423.7	0.3848; 4.3229; 13.3235	
$\pm m_J$ states (from 21 sextets+ 108 Quartets only)	$g_{xx}; g_{yy}; g_{zz}$	$\theta(^{\circ}$ angle)
0.0	0.0009; 0.0022; 19.8783	0
239.4	1.8180; 2.0794; 14.7238	3.2
264.9	0.1919; 2.1447; 13.5704	86.9
286.8	1.3198; 1.6613; 12.4955	88.7
344.8	0.3187; 3.3590; 10.6326	94.6
367.0	10.0847; 6.3812; 2.0309	93.8
401.8	1.6317; 3.1583; 12.4591	67.8
417.1	0.3960; 4.2481; 13.3108	41.7

Table S11. SINGLE_ANISO computed wavefunction decomposition analysis for Dy1 centre

and Dy2 centre in complex **1**. The major dominating values are kept in bold.

$\pm m_J$	<i>wave function decomposition analysis Dy1</i>
KD1	96.8% $ \pm 15/2\rangle$ + 1.2% $ \pm 11/2\rangle$
KD2	78.5% $ \pm 13/2\rangle$ + 12.7% $ \pm 1/2\rangle$ + 2.8% $ \pm 5/2\rangle$ + 1.2% $ \pm 9/2\rangle$
KD3	64.7% $ \pm 1/2\rangle$ + 12.2% $ \pm 13/2\rangle$ + 3.1% $ \pm 3/2\rangle$ + 1.4% $ \pm 9/2\rangle$
KD4	40.1% $ \pm 3/2\rangle$ + 8.8% $ \pm 5/2\rangle$ + 3.4% $ \pm 5/2\rangle$ + 3.1% $ \pm 7/2\rangle$ + 1.3% $ \pm 1/2\rangle$
KD5	55.5% $ \pm 5/2\rangle$ + 5.1% $ \pm 5/2\rangle$ + 3.4% $ \pm 3/2\rangle$ + 3.2% $ \pm 11/2\rangle$ + 2.3% $ \pm 1/2\rangle$ + 1.6% $ \pm 7/2\rangle$
KD6	53.2% $ \pm 11/2\rangle$ + 23.5% $ \pm 7/2\rangle$ + 3.4% $ \pm 3/2\rangle$ + 2.2% $ \pm 5/2\rangle$
KD7	41.8% $ \pm 7/2\rangle$ + 18.7% $ \pm 11/2\rangle$ + 2.4% $ \pm 5/2\rangle$ + 1.9% $ \pm 3/2\rangle$ + 1.2% $ \pm 9/2\rangle$
KD8	68.7% $ \pm 9/2\rangle$ + 5.5% $ \pm 7/2\rangle$ + 4.1% $ \pm 11/2\rangle$ + 3.7% $ \pm 5/2\rangle$ + 1.2% $ \pm 1/2\rangle$
$\pm m_J$	<i>wave function decomposition analysis Dy2</i>
KD1	97.2% $ \pm 15/2\rangle$ + 1.1% $ \pm 11/2\rangle$
KD2	75.1% $ \pm 13/2\rangle$ + 12.6% $ \pm 1/2\rangle$ + 2.8% $ \pm 5/2\rangle$ + 1.2% $ \pm 9/2\rangle$
KD3	50.2% $ \pm 1/2\rangle$ + 11.8% $ \pm 13/2\rangle$ + 7.6% $ \pm 3/2\rangle$ + 1.1% $ \pm 9/2\rangle$
KD4	44.1% $ \pm 3/2\rangle$ + 7.8% $ \pm 1/2\rangle$ + 2.9% $ \pm 7/2\rangle$ + 2.1% $ \pm 5/2\rangle$ + 1.1% $ \pm 13/2\rangle$
KD5	46.1% $ \pm 5/2\rangle$ + 4.6% $ \pm 9/2\rangle$ + 4.3% $ \pm 3/2\rangle$ + 3.1% $ \pm 1/2\rangle$ + 2.4% $ \pm 7/2\rangle$
KD6	54.1% $ \pm 11/2\rangle$ + 25.4% $ \pm 7/2\rangle$ + 3.1% $ \pm 3/2\rangle$ + 2.2% $ \pm 5/2\rangle$
KD7	45.3% $ \pm 7/2\rangle$ + 21.3% $ \pm 11/2\rangle$ + 2.4% $ \pm 5/2\rangle$ + 2.6% $ \pm 3/2\rangle$ + 1.3% $ \pm 9/2\rangle$
KD8	48.1% $ \pm 9/2\rangle$ + 6.5% $ \pm 7/2\rangle$ + 3.2% $ \pm 11/2\rangle$ + 2.4% $ \pm 5/2\rangle$ + 1.1% $ \pm 1/2\rangle$

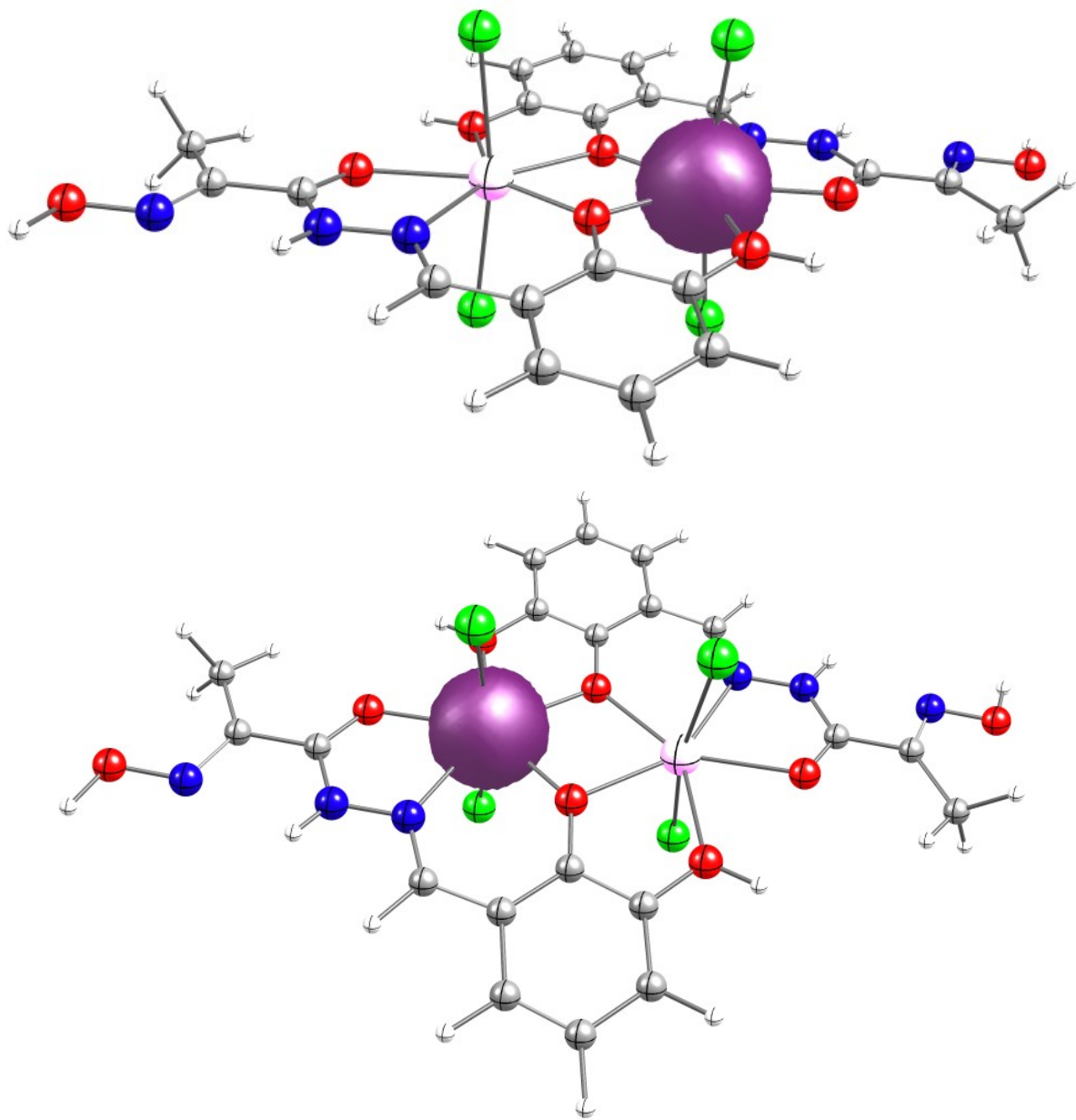


Figure S11. CASSCF computed beta state spin-density of both Dy1 and Dy2 centers in complex **1**. The iso-density surface represented here corresponds to an value of 0.001 e⁻/bohr³. The violet and yellow color indicate positive and negative spin densities respectively.

Table S12. SINGLE_ANISO computed crystal field parameters for Dy1 and Dy2 centres in complex **1**. The major dominating values are kept in bold.

k	q	B_k^q	B_k^q
		Dy1	Dy2
2	-2	0.93E+00	-0.64E+00
	-1	0.52E+00	0.39E+00
	0	-0.31E+01	-0.31E+01
	2	-0.33E+00	0.46E+00
	1	-0.10E+01	0.10E+01
4	-4	-0.75E-01	-0.73E-01
	-3	-0.14E-01	0.38E-01
	-2	0.11E-02	0.29E-02
	-1	-0.24E-02	-0.81E-02
	0	-0.60E-01	-0.60E-01
	1	0.91E-02	-0.26E-02
	2	-0.24E-01	0.25E-01
	3	0.35E-01	0.39E-02
	4	-0.11E-01	0.16E-01
6	-6	-0.38E-03	0.19E-02
	-5	0.13E-02	0.67E-03
	-4	-0.75E-03	-0.87E-03
	-3	-0.21E-03	0.31E-03
	-2	-0.49E-03	0.54E-03
	-1	-0.46E-03	0.43E-03
	0	-0.88E-05	-0.10E-04
	1	-0.49E-03	-0.50E-03
	2	-0.34E-03	0.26E-03
	3	0.25E-03	0.13E-03
	4	-0.43E-03	-0.15E-03
	5	-0.10E-03	0.11E-02
	6	-0.30E-02	0.24E-02

Table S13. CASSCF computed LoProp charges for complex **1**. The atoms in bold represent first coordinating seven atoms around Dy1 and Dy2 centers.

Dy1 center		Dy2 center	
Dy1	2.4527	Lu1	1.3073
Lu2	1.3072	Dy2	2.4528
Cl3	-0.8538	Cl3	-0.6253
Cl4	-0.8556	Cl4	-0.6299

O5	-0.7743	O5	-0.7548
O6	-0.6687	O6	-0.5448
O7	-0.4409	O7	-0.5476
N8	-0.2753	N8	-0.1506
N9	-0.1540	N9	-0.1562
O10	-0.4002	O10	-0.4001
N11	-0.0747	N11	-0.0749
C12	-0.0830	C12	-0.0825
C13	0.1275	C13	0.1318
C14	0.5022	C14	0.5071
C15	-0.0858	C15	-0.0892
C16	-0.1235	C16	-0.1237
C17	0.2930	C17	0.2926
C18	-0.1056	C18	-0.1065
C19	0.1801	C19	0.1814
C20	0.1165	C20	0.1191
C21	-0.3085	C21	-0.3087
Cl22	-0.6251	Cl22	-0.8536
Cl23	-0.6298	Cl23	-0.8555
O24	-0.7546	O24	-0.7743
O25	-0.5410	O25	-0.6646
O26	-0.5474	O26	-0.4408
N27	-0.1555	N27	-0.2806
N28	-0.1716	N28	-0.1692
H29	0.2579	H29	0.2557
O30	-0.3995	O30	-0.3995
N31	-0.0710	N31	-0.0709
C32	-0.0822	C32	-0.0827
C33	0.1311	C33	0.1269
C34	0.5115	C34	0.5066
C35	-0.0895	C35	-0.0861
C36	-0.1239	C36	-0.1236
C37	0.2931	C37	0.2934
C38	-0.1061	C38	-0.1052
C39	0.1814	C39	0.1801
C40	0.1156	C40	0.1130
C41	-0.3087	C41	-0.3085
H42	0.2481	H42	0.2502
H43	0.3453	H43	0.3453
H44	0.1049	H44	0.1048
H45	0.1003	H45	0.1019
H46	0.1133	H46	0.1132
H47	0.1124	H47	0.1125
H48	0.1320	H48	0.1321
H49	0.1344	H49	0.1348
H50	0.1319	H50	0.1320
H51	0.3460	H51	0.3459
H52	0.1050	H52	0.1052
H53	0.1035	H53	0.1020
H54	0.1133	H54	0.1133

H55	0.1126	H55	0.1125
H56	0.1320	H56	0.1318
H57	0.1344	H57	0.1340
H58	0.1320	H58	0.1318
H59	0.3709	H59	0.3678
H60	0.3679	H60	0.3711

Table S14. BS-DFT computed energies of high-spin and broken-symmetry solution of Gd analogue of complex **1** using $H = -JS_1S_2$ formalism. All J values are provided in cm^{-1} .

Complex	Solution	Energy (E_h)	$\rho^{\text{Gd1}}, \rho^{\text{Gd2}}$	$\langle S^{**2} \rangle$	J_{GdGd}	$J_{\text{Dy-Dy}} \\ [(49/25) * J_{\text{Gd-Gd}}]$
1	HS	-26076.347538	7.0316 7.0321	56.0133	-0.21	-0.42
	BS	-26076.347586	7.0313 -7.0317	7.0132		

Table S15. Cartesian coordinates of complex **1** with optimized hydrogens only.

Dy	1.601376	4.104535	12.573378
Dy	3.143834	1.604482	10.346868
Cl	1.727360	6.007249	10.789611
Cl	1.305844	2.520915	14.647280
O	1.087629	2.500827	11.026222
O	0.603988	5.738506	13.935032
O	1.344378	0.547038	9.265417
N	-0.850866	4.153443	12.432408
N	-1.428293	5.141805	13.197800
O	-3.128789	8.003046	15.365621
N	-2.560631	7.003264	14.627724
C	-2.451622	1.519475	10.498529
C	-1.671901	3.355740	11.844911
C	-0.638531	5.912078	13.934250
C	-1.345728	2.253265	10.992226
C	-2.293858	0.483218	9.641165
C	-0.048332	1.910850	10.596486
C	-1.018740	0.131675	9.231655
C	0.066690	0.841510	9.658866
C	-1.267238	6.996317	14.740889
C	-0.448158	7.943504	15.532410
Cl	3.017849	-0.298233	12.130635
Cl	3.439366	3.188102	8.272966
O	3.657581	3.208190	11.894024
O	4.141222	-0.029490	8.985214

O	3.400831	5.161979	13.654829
N	5.596076	1.555574	10.487838
N	6.173504	0.567211	9.722445
H	7.194320	0.423959	9.690374
O	7.873999	-2.294030	7.554626
N	7.305840	-1.294247	8.292523
C	7.196832	4.189541	12.421718
C	6.417111	2.353277	11.075336
C	5.383740	-0.203062	8.985995
C	6.090938	3.455752	11.928019
C	7.039067	5.225799	13.279081
C	4.793541	3.798167	12.323760
C	5.763950	5.577341	13.688591
C	4.678519	4.867506	13.261380
C	6.012448	-1.287300	8.179357
C	5.193367	-2.234487	7.387835
H	-2.449516	5.284624	13.229297
H	-4.087231	7.897962	15.202891
H	-3.458951	1.817876	10.829287
H	-2.762946	3.510440	11.999118
H	-3.162047	-0.085409	9.277127
H	-0.870751	-0.711581	8.535598
H	-0.562971	8.973814	15.134848
H	0.616304	7.654685	15.494490
H	-0.794456	7.969281	16.585808
H	8.832445	-2.188920	7.717317
H	8.204164	3.891160	12.090954
H	7.508125	2.198538	10.921057
H	7.907249	5.794427	13.643134
H	5.616004	6.420681	14.384536
H	5.308300	-3.264822	7.785295
H	4.128893	-1.945721	7.425817
H	5.539579	-2.260154	6.334404
H	1.371551	-0.191274	8.626807
H	3.372965	5.896322	14.297934